Research Article

Investigation into the Influence of Substitutions on the Structural Characteristics of Sr_2FeMoO_6

Vugar H. Mirzayev[1] and Dilmurod A. Rakhmanov[2]

[1]National University of Uzbekistan named after Mirzo Ulugbek, 20 Yangi Almazar Street, 100057 Tashkent, Uzbekistan
[2]Institute of Semiconductor Physics and Microelectronics, National University of Uzbekistan, 20 Yangi Almazar Street, 100057 Tashkent, Uzbekistan

Received: 05.11.2025 Accepted: 09.11.2025 Published: 19.11.2025

https://doi.org/10.54414/XVZB1367

Abstract

Sr_2FeMoO_6 is a half-metallic ferromagnet with a high Curie temperature, which positions it as a strong candidate for spintronic devices. Its lattice features ordered Fe and Mo cations on the B sites, and this arrangement underpins distinctive electronic transport and robust magnetic exchange. Here we examine Sr_2FeMoO_6 and the substituted phases $Sr_2FeMo_{1-x}Ta_xO_6$ with x = 0.05 and $Sr_2FeMo_{1-x}V_xO_6$ with x = 0.15 by neutron diffraction across multiple temperatures. The data show that temperature and B-site substitution drive measurable changes in unit-cell metrics and anisotropy. These results clarify the structural and thermal responses of this double perovskite family and inform their use in technology.

Keywords: neutron diffraction, rietveld refinement, substitutions, low temperature

1. Introduction

Sr_2FeMoO_6 is a double perovskite oxide that exhibits half-metallic ferromagnetism together with a high Curie temperature, which makes it a strong candidate for spintronic devices. Its lattice hosts an ordered arrangement of Fe and Mo cations on the B sites, and this chemical ordering drives unusual electronic transport and robust magnetic exchange. As a result, the material combines near-perfect spin polarization with stable long-range magnetism at technologically relevant temperatures [1]. Furthermore, Sr_2FeMoO_6 has been explored for applications in solid oxide fuel cells due to its strong electronic conductivity and thermal resilience [2].

Sr_2FeMoO_6 is a B-site-ordered double perovskite that combines highly spin-polarized conduction with stable ferrimagnetic behavior at and above room temperature. Its magnetic and electronic performance originates from the distinctive interaction between Fe and Mo ions and the resulting band structure [3]. Achieving high magnetization, strong spin polarization, and reliable transport properties depends on strict control of composition, oxygen non-stoichiometry, and cation ordering in both bulk samples and thin film architectures [4]. Because its defect chemistry can be adjusted over a wide range, Sr_2FeMoO_6 serves as a flexible material platform for spintronic elements and magnetoresistive devices used in oxide-based electronics [5]. Tailored microstructures and composite configurations also produce strong responses in the radio frequency and microwave regimes, which makes the material useful for sensing technologies and electromagnetic interference management [6]. In addition to these functions, the combined electrical conductivity, redox durability, and ability to accommodate dopants make Sr_2FeMoO_6 a promising option for electrocatalytic applications and as an anode material in solid oxide electrochemical systems [1].

Sr_2FeMoO_6 is a B-site ordered double perovskite that shows half-metallicity and robust ferrimagnetism near room temperature. Large low-field magnetoresistance arises from spin-polarized tunneling across grain

boundaries. This result established SFMO as a model oxide for spintronics [7]. Neutron diffraction and magnetometry confirm ferrimagnetic ordering arising from Fe^{3+}–O–Mo^{5+} pathways in ordered SFMO and reveal how even modest Fe/Mo antisite disorder measurably depresses the refined magnetic moments and transition temperature [8]. Room-temperature neutron data on SFMO–δ ceramics underscore that oxygen-defect chemistry subtly distorts the cell and modulates ordered moments, reinforcing the tight coupling among oxygen content, structural metrics, and ferri-magnetic order [9].

The study [10] revealed that increasing the total sintering time significantly improved Fe/Mo cation ordering in Sr_2FeMoO_6, reducing antisite defects and increasing the degree of ordering from 44.9% to 80.2%. Rietveld refinement showed a gradual decrease in unit cell volume and bond lengths (Fe–O and Mo–O) with extended sintering, indicating a more compact and ordered crystal structure. Additionally, the Fe–O1–Mo bond angle increased with sintering time, reflecting reduced octahedral tilting and enhanced linearity along the Fe–O–Mo chains. A structural phase transition from cubic ($Fm\bar{3}m$) to tetragonal ($I4/m$) symmetry occurs in Sr_2FeMoO_6 near 400 K, accompanied by octahedral rotations and the onset of ferrimagnetic ordering. Neutron diffraction and Mössbauer spectroscopy revealed a saturated Fe magnetic moment of ~4.3 μB and an intermediate Fe valence state, with approximately 6% Mo-site vacancies contributing to local structural and magnetic inhomogeneity [11]. Cation ordering in the $I4/m$ structure and antisite defects control the balance between high saturation magnetization, metallic transport, and spin polarization. Targeted A- or B-site substitutions and careful oxygen control tune the Curie temperature and magnetoresistance. This review frames the structure–property rules that guide later work [12]. Systematic neutron refinements of $Sr_2Fe_{0.75}T_{0.25}MoO_6$ (T = Cr, Mn, Co, Ni) demonstrate dopant-specific lattice distortions and disorder that degrade M_s and metallicity to differing degrees, mapping how 3d-dopant chemistry perturbs Fe–O–Mo exchange [13]. In $Sr_2Fe_{1-x}Cr_xMoO_{6-\gamma}$, increasing Cr systematically reduces M_s and increases resistivity by disrupting Fe–O–Mo double-exchange and promoting antisites/oxygen defects, providing a clear, composition-dependent picture of structure–magnetism coupling [14].

Magnetocaloric measurements on SFMO and W-doped analogs link structural distortions to the magnetic-entropy change, indicating that judicious B-site chemistry can shift operating windows toward technologically relevant temperatures [15].

In this context, our research focuses on further understanding the structural behavior of Sr_2FeMoO_6-based systems under different doping strategies and temperature conditions using high-resolution neutron diffraction and Rietveld analysis.

2. Research Method

Neutron diffraction measurements were conducted over a range of temperatures using the High-Resolution Fourier Diffractometer (HRFD) at the Frank Laboratory of Neutron Physics, Joint Institute for Nuclear Research (JINR), Dubna, Russia. The instrument provides high angular resolution and is optimized for the precise determination of lattice parameters and atomic positions, allowing accurate tracking of temperature-induced structural variations in the studied samples [16]. The purpose was to investigate the structural behavior of the parent compound Sr_2FeMoO_6 and its cation-substituted derivatives, namely $Sr_2FeMo_{1-x}Ta_xO_6$ (x = 0.05) and $Sr_2FeMo_{1-x}V_xO_6$ (x = 0.15). Samples were synthesized with controlled stoichiometry and uniform microstructure to ensure reliable diffraction data. Temperature and B-site substitution with Ta and V were varied systematically to assess their impact on unit-cell metrics. Lattice parameters were obtained by full-profile Rietveld refinement, which also yielded fit statistics and peak-broadening indicators. These measurements provide a consistent basis for interpreting thermal and substitution effects in this double perovskite system [17,18].

3. Results and Discussion

Neutron diffraction experiments were conducted on Sr_2FeMoO_6-based samples at varying dopant concentrations and temperatures. The diffraction spectra were refined using the Rietveld method implemented in the FullProf Suite software [19,20].

In the initial undoped state, the diffraction pattern illustrates a well-defined structure, from which changes in lattice parameters with temperature were identified (Figure 1).

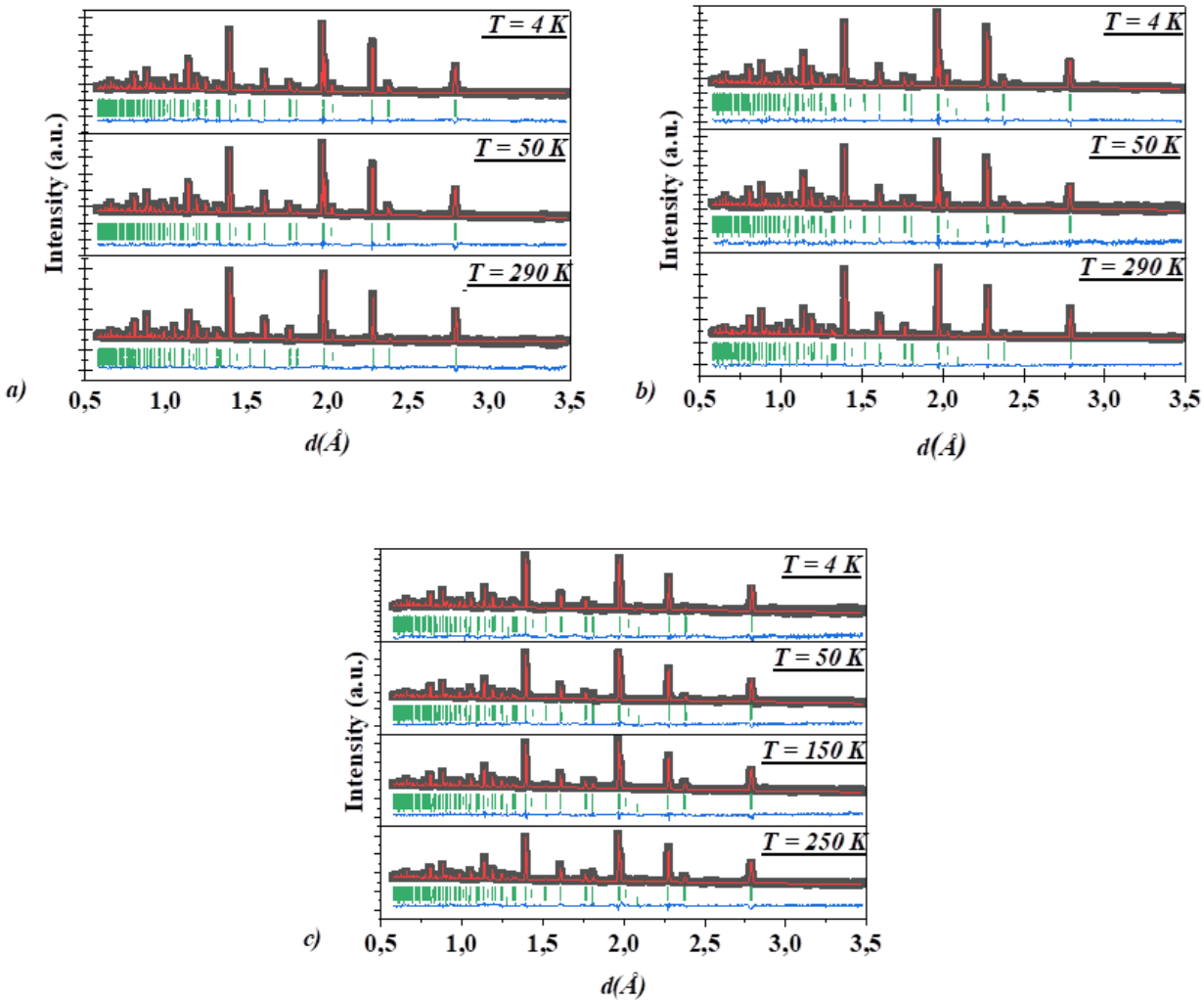

Figure 1. Neutron diffraction patterns of (a) initial **Sr_2FeMoO_6,** (b) **$Sr_2FeMo_{1-x}V_xO_6$** (x = 0.15), and (c) **$Sr_2FeMo_{1-x}Ta_xO_6$** (x = 0.05) at different temperatures. Black dots represent experimental data, the red line is the Rietveld refinement fit, green vertical ticks indicate Bragg reflection positions, and the blue line shows the difference between observed and calculated intensities.

Following V doping at x = 0.15, diffraction patterns were collected at three temperatures, as shown in Fig. 1b. In addition to the perovskite reflections, weak extra peaks appear that do not index to the Sr_2FeMoO_6 cell and are assigned to aluminum and copper from the sample environment used to secure the containers under the measurement conditions. In the Ta doped compound $Sr_2FeMo_{1-x}Ta_xO_6$ with x = 0.05, the unit cell volume remains close to that of the undoped sample, with a slight increase at intermediate temperature and reaching 245.95 Å^3 at 250 K as shown in Fig. 1c. The a axis shows a minor expansion while the c axis is nearly temperature independent, which indicates that the framework is largely preserved with Ta substitution. The full set of refined structural parameters is summarized in Table 1. For the undoped Sr_2FeMoO_6, the unit cell volume increases with temperature from 244.63 Å^3 at 4 K to 246.14 Å^3 at 290 K, consistent with moderate thermal expansion.

For the V-doped composition $Sr_2FeMo_{1-x}V_xO_6$ with x equal to 0.15, the unit cell volume remains smaller at all temperatures when compared with the undoped material and the Ta-substituted sample [21]. At 4 K, the volume reaches its lowest value of 243.99 Å^3. The c-axis shows the strongest decrease, which indicates that the

introduction of vanadium produces a clear lattice contraction. This shrinkage is more evident than the effect produced by Ta substitution and demonstrates the stronger structural impact of vanadium on the Sr_2FeMoO_6 lattice.

Table 1. The changes in structural parameters after substitution.

Space group I 4/m m m	a	c	V
Sr_2FeMoO_6 T = 4 K	5.5599(1)	7.9134(1)	244.627(6)
Sr_2FeMoO_6 T = 50 K	5.5607(1)	7.9138(2)	244.71(1)
Sr_2FeMoO_6 T = 290 K	5.5785(1)	7.9096(2)	246.14(1)
$Sr_2FeMo_{1-x}V_xO_6$ x=0.15, T = 4 K	5.5560(1)	7.9040 (2)	243.994 (1)
$Sr_2FeMo_{1-x}V_xO_6$ x=0.15, T = 50 K	5.5547(1)	7.9039(2)	243.98(1)
$Sr_2FeMo_{1-x}V_xO_6$ x=0.15, T = 290 K	5.5730(1)	7.8986(2)	245.32(1)
$Sr_2FeMo_{1-x}T_{ax}O_6$ x=0.05, T = 4 K	5.5628 (2)	7.9059(2)	244.778(2)
$Sr_2FeMo_{1-x}Ta_xO_6$ x=0.05, T = 50 K	5.5628(2)	7.9101(3)	244.78(1)
$Sr_2FeMo_{1-x}Ta_xO_6$ x=0.05, T = 150 K	5.5676 (2)	7.9085 (3)	245.15(2)
$Sr_2FeMo_{1-x}TaxO_6$ x=0.05, T = 250 K	5.576(1)	7.909(1)	245.95(5)

These findings emphasize the role of B-site substitution in tuning the thermal and structural behavior of double perovskites. While Ta maintains structural integrity across temperature ranges, V leads to distinct lattice shrinkage, underlining the importance of dopant selection for potential applications where thermal and structural stability are critical.

4. Conclusion

Taken together, the results show that temperature and B-site substitution strongly govern the crystal structure of Sr_2FeMoO_6. Thermal expansion increases the unit-cell volume of the pristine compound, and the effect is anisotropic along the a and c axes. Ta incorporation keeps the lattice essentially unchanged and points to good structural robustness under heating. V substitution produces a clear lattice contraction, most notably along the c axis, consistent with a modified bonding environment and altered octahedral distortions. These insights identify B-site chemistry as an effective handle to tailor thermal and structural responses in double perovskites, and they guide optimization for spintronic and solid-oxide energy applications.

Author Contributions

Dilmurod A. Rakhmanov: conceptualization methodology, writing original draft.

Vugar H. Mirzayev: conceptualization, funding, acquisition, project administration.

Funding

No funding was received for this research.

Conflicts of Interest

The authors declare that they have no conflicts of interest.

Supplementary Information

Not applicable.

Ethical Approval

Not applicable.

Acknowledgments

The authors thank A.S. Abiyev for his assistance in conducting the experiment.

Data and Code Availability

The data supporting the findings of this study are available from the corresponding author upon reasonable request. No custom code was used in this study.

Abbreviations

Strontium Iron Molybdate (Sr_2FeMoO_6), Iron (Fe), Molybdenum (Mo), Strontium Iron Molybdenum Tantalum Oxide ($Sr_2FeMo_{1-x}Ta_xO_6$), Strontium Iron Molybdenum Vanadium Oxide ($Sr_2FeMo_{1-x}V_xO_6$), SFMO (Sr_2FeMoO_6), Chromium (Cr), Manganese (Mn), Cobalt (Co), Nickel (Ni), Saturation Magnetization (M_s) High Resolution Fourier Diffractometer (HRFD), Joint Institute for Nuclear Research (JINR).

References

1. Liao, Y., Xi, X., Chen, H., Liu, J., Fu, X. Z., & Luo, J. L. (2024). The emerging Sr2FeMoO6-based electrocatalysts for solid oxide electrochemical cell: synthesis, modulation and applications. https://doi.org/10.20517/cs.2023.47
2. Suchaneck, G., Kalanda, N., Yarmolich, M., Artiukh, E., Gerlach, G., & Sobolev, N. A. (2022). Magnetization of magnetically inhomogeneous Sr2FeMoO6-δ nanoparticles. *Electronic Materials*, *3*(1), 82-92. https://doi.org/10.29003/m3067.mmmsec-2022/58-58
3. Sarma, D. D., Mahadevan, P., Saha-Dasgupta, T., Ray, S., & Kumar, A. (2000). Electronic Structure of Sr 2 FeMoO 6. *Physical review letters*, *85*(12), 2549. https://doi.org/10.1103/physrevlett.85.2549
4. Hauser, A. J., Williams, R. E., Ricciardo, R. A., Genc, A., Dixit, M., Lucy, J. M., & Yang, F. (2011). Unlocking the potential of half-metallic Sr 2 FeMoO 6 films through controlled stoichiometry and double-perovskite ordering. *Physical Review B—Condensed Matter and Materials Physics*, *83*(1), 014407. https://doi.org/10.1103/physrevb.83.014407
5. Sarma, D. D. (2001). A new class of magnetic materials: Sr2FeMoO6 and related compounds. *Current Opinion in Solid State and Materials Science*, *5*(4), 261-268. https://doi.org/10.1016/s1359-0286(01)00014-6
6. Das, R., Chaudhuri, U., & Mahendiran, R. (2021). Microwave magnetoresistance and microwave absorption in Sr2FeMoO6. *ACS Applied Electronic Materials*, *3*(7), 3072-3078. https://doi.org/10.1021/acsaelm.1c00304
7. Kobayashi, K. I., Kimura, T., Sawada, H., Terakura, K., & Tokura, Y. (1998). Room-temperature magnetoresistance in an oxide material with an ordered double-perovskite structure. *Nature*, *395*(6703), 677-680. https://doi.org/10.1038/27167
8. Chung, M. K., Huang, P. J., Li, W. H., Yang, C. C., Chan, T. S., Liu, R. S., & Lynn, J. W. (2006). Crystalline and magnetic structures of Sr2FeMoO6 double perovskites. *Physica B: Condensed Matter*, *385*, 418-420. https://doi.org/10.1016/j.physb.2006.05.140
9. Sikolenko, V., Kalanda, N., Yarmolich, M., Petrov, A., Karpinsky, D., Efimov, V., & Savvin, S. (2025). Neutron Diffraction Study of the Magnetic Structure of Sr2FeMoO6–δ. *Physics of Particles and Nuclei Letters*, *22*(5), 1278-1282. https://doi.org/10.1134/s1547477125701559
10. Hu, Y. C., Ge, J. J., Ji, Q., Lv, B., Wu, X. S., & Cheng, G. F. (2010). Synthesis and crystal structure of double-perovskite compound Sr2FeMoO6. *Powder Diffraction*, *25*(S1), S17-S21. https://doi.org/10.1154/1.3478711
11. Chmaissem, O., Kruk, R., Dabrowski, B., Brown, D. E., Xiong, X., Kolesnik, S., & Kimball, C. W. (2000). Structural phase transition and the electronic and magnetic properties of Sr 2 FeMoO 6. *Physical Review B*, *62*(21), 14197. https://doi.org/10.1103/physrevb.62.14197

12. Serrate, D., De Teresa, J. M., & Ibarra, M. R. (2006). Double perovskites with ferromagnetism above room temperature. *Journal of Physics: Condensed Matter*, *19*(2), 023201. https://doi.org/10.1088/0953-8984/19/2/023201
13. Ritter, C., Blasco, J., De Teresa, J. M., Serrate, D., Morellon, L., Garcia, J., & Ibarra, M. R. (2004). Structural and magnetic details of 3d-element doped Sr2Fe0. 75T0. 25MoO6. *Solid state sciences*, *6*(5), 419-431. https://doi.org/10.1016/j.solidstatesciences.2004.02.007
14. Blasco, J., Ritter, C., Morellon, L., Algarabel, P. A., De Teresa, J. M., Serrate, D., & Ibarra, M. R. (2002). Structural, magnetic and transport properties of Sr2Fe1− xCrxMoO6− y. *Solid state sciences*, *4*(5), 651-660. https://doi.org/10.1016/s1293-2558(02)01309-2
15. Zhong, W., Liu, W., Wu, X. L., Tang, N. J., Chen, W., Au, C. T., & Du, Y. W. (2004). Magnetocaloric effect in the ordered double perovskite Sr2FeMo1− xWxO6. *Solid state communications*, *132*(3-4), 157-162. https://doi.org/10.1016/j.ssc.2004.07.060
16. Hasanov, K. M., Abiyev, A. S., Sumnikov, S. V., Kostishyn, V. G., Trukhanov, A. V., Trukhanov, S. V., & Turchenko, V. A. (2025). Effects of Non-Isovalent Substitution on the Structural and Magnetic Properties of SrFe12-x (CoSn) xO19 Solid Solutions (x= 0–0.5). *Journal of Alloys and Compounds*, 182512. https://doi.org/10.1016/j.jallcom.2025.182512
17. Abiyev, A. S., Samadov, S. F., Mehdiyeva, R. N., Dadashzade, G. A., Kvasovich, E. O., & Huseynov, E. M. (2025). Oxidation dynamics in gamma-irradiated TiN nanoparticles after annealing. *Ceramics International*. https://doi.org/10.1016/j.ceramint.2025.04.019
18. Abiyev, A. S. (2021). Physicochemical processes in aluminum nanoparticles at high temperatures. *Advanced Physical Research*, *3*(3), 137-141. https://doi.org/10.4028/www.scientific.net/amr.872.248
19. Samadov, S. F., Samedov, O. A., Mirzayeva, D. M., Nguyen, H. H. A., & Mirzayev, M. N. (2025). Effect of gamma irradiation and thermal annealing on defect formation in ZrB2 nanocrystals. *Physica B: Condensed Matter*, 417807. https://doi.org/10.1016/j.physb.2025.417807
20. Samadov, S. F., Abiyev, A. S., Asadov, A. G., Trung, N. V. M., Sidorin, A. A., Samedov, O. A., & Mirzayev, M. N. (2024). Investigating the crystal structure of ZrB2 under varied conditions of temperature, pressure, and swift heavy ion irradiation. *Ceramics International*, *50*(2), 3727-3732. https://doi.org/10.1016/j.ceramint.2023.11.125
21. Abdullayev, A. P., Samadov, S. F., Abiyev, A. S., Sidorin, A. A., Trung, N. V. M., Orlov, O. S., & Musazade, I. V. (2025). Defect and crystal structure variation in Tl-doped TlGaTe2 semiconductor alloys: An experimental and theoretical study. *Journal of Alloys and Compounds*, *1038*, 182773. https://doi.org/10.1016/j.jallcom.2025.182773